Aust. J. Phys., 1988, **41**, 173–87

Profile Analysis for Microcrystalline Properties by the Fourier and Other Methods*

J. I. Langford,[A] *R. Delhez,*[B] *Th.H. de Keijser*[B] *and E. J. Mittemeijer*[B]

[A] Department of Physics, University of Birmingham, Birmingham B15 2TT, U.K.
[B] Laboratory of Metallurgy, Delft University of Technology, 2628 AL Delft, The Netherlands.

Abstract

In the 1960s the Fourier and variance methods superseded the use of the FWHM and integral breadth in detailed studies of microcrystalline properties. Provided that due allowance is made in the analysis for systematic errors, particularly the effects of truncation of diffraction line profiles at a finite range, these remain the best methods for characterising crystallite size and shape, microstrains and other imperfections in cases where accuracy is important. However, the application of the Fourier, variance and related methods in general requires that the diffraction lines are well resolved and it is thus restricted to materials with high symmetry or which exhibit a high degree of preferred orientation. Most materials, on the other hand, including many of technological importance, have complex patterns with severe overlapping of peaks. The introduction of pattern-decomposition methods, whereby a suitable model is fitted to the total diffraction pattern to give profile parameters for individual lines, means that microcrystalline properties can now be studied for any crystalline material or mixture of substances. The use of the FWHM and integral breadth has been given a new lease of life; though the information is less detailed than is given by the Fourier and variance methods and systematic errors are in general greater, self-consistent estimates of crystallite size and microstrains are obtained.

At present the most promising technique for analysing the breadths obtained from pattern decomposition is the Voigt method applied to all lines of a diffraction pattern. When *reliable* data for two or more orders of reflections are available, a multiple-line analysis can be used to separate the contributions to line breadths from crystallite size and strain. For other reflections a single-line approach is used, though this can introduce an angle-dependent systematic error.

1. Introduction: A Historical Overview

The use of diffraction line profiles to study microcrystalline properties is almost as old as powder diffraction itself. As long ago as 1918 Scherrer noted that the line breadth varied inversely as the size ϵ of crystallites in the sample, leading to the Scherrer equation

$$\beta = \lambda/\epsilon \cos\theta \quad \text{for breadths on a } 2\theta \text{ scale} \tag{1a}$$

or

$$\beta = 1/\epsilon \quad \text{for breadths in reciprocal units,} \tag{1b}$$

where λ is the wavelength, θ is the Bragg angle and β is some measure of line

* Paper presented at the International Symposium on X-ray Powder Diffractometry, held at Fremantle, Australia, 20–23 August 1987.

0004-9506/88/020173$03.00

breadth. In (1) ϵ is an apparent size which depends on the measure of breadth used, the shape of the crystallites and the direction of the *hkl* planes, and it is related to the true size through the Scherrer constant. From (1) it is evident that size broadening is independent of the order of a reflection. The broadening which arises from microstrains was reported by Van Arkel in 1925, but its cause was the subject of controversy for many years and the description of line-profile shape for a specimen containing a distribution of microstrains is still a matter of debate (Delhez *et al.* 1982; Delhez *et al.* 1988, present issue p. 213). Various early workers deduced the angular dependence of strain broadening and the forms normally used are as follows:

(i) The microstrain $\tilde{e}$ is conceived by considering two extreme values of the lattice spacing d, namely $d+\Delta d$ and $d-\Delta d$, with $\tilde{e} = \Delta d/d$. By equating the integral breadth β with the angular range corresponding to $d+\Delta d$ and $d-\Delta d$, and by assuming that Bragg's law holds over this range (implying that parts of the specimen with spacings $d-\Delta d$ and $d+\Delta d$ diffract independently, i.e. *incoherently*), we have

$$\beta = 4\tilde{e}\tan\theta \quad \text{for a } 2\theta \text{ scale} \tag{2a}$$

or

$$\beta = 4\tilde{e}/2d \quad \text{in reciprocal units } (1/d \text{ scale}). \tag{2b}$$

(ii) The component of strain $e(n)$ denotes the average strain between two unit cells, n cells apart, in a column of cells perpendicular to the diffracting planes. For a Gaussian distribution of $e(n)$, independent of the separation of cells n [implying that $\langle e^2(n)\rangle = \langle e^2\rangle$, the mean-square strain], a Gaussian strain profile is obtained. The region which includes the variation in lattice spacing is now considered as diffracting *coherently* and (Stokes and Wilson 1944)

$$\beta = 2(2\pi)^{\frac{1}{2}}\langle e^2\rangle^{\frac{1}{2}}\tan\theta = 5\langle e^2\rangle^{\frac{1}{2}}\tan\theta \quad \text{for a } 2\theta \text{ scale} \tag{2c}$$

or

$$\beta = 2(2\pi)^{\frac{1}{2}}\langle e^2\rangle^{\frac{1}{2}}/2d = 5\langle e^2\rangle^{\frac{1}{2}}/2d \quad \text{in reciprocal units}. \tag{2d}$$

Equations (2) indicate that strain broadening depends on the order of a reflection.

In 1949 Hall proposed a method for separating size and strain effects by plotting the breadths of reciprocal lattice points against their distance from the origin. The intercept is then $1/\epsilon$ and the slope is proportional to the strain. He further developed this approach with Williamson to form the basis of the Williamson–Hall (1953) plot.

Experimental h line profiles are the convolution of the specimen f and instrumental g contributions, and the f profiles in turn can be the convolution of several functions which are grouped together as the order-independent ('size') and order-dependent ('strain') contributions, or

$$h(x) = f_S(x) \star f_D(x) \star g(x), \tag{3}$$

where S and D denote 'size' and 'strain'. For ease of deconvolution of the various components, early work on line-broadening analysis was based on the assumption that the constituent line profiles are either Cauchy (Lorentzian) or Gaussian. It was evident that neither function accurately models experimental profiles and that a

more rigorous approach would be to use the multiplicative property of the Fourier transforms of convoluted functions, or

$$H(t) = F(t)\,G(t), \tag{4}$$

where F, G, H are Fourier transforms of f, g, h. This milestone in the development of line-broadening analysis led to the Stokes (1948) correction for instrumental broadening and the Warren–Averbach (1949, 1950) method for the separation of size and strain effects by using the Fourier coefficients of the pure diffraction profile. An alternative procedure to overcome the problems associated with deconvolution, suggested by Tournarie (1956) and developed by Wilson (1962) and Langford (1965), is to use the additive property of the variances (second central moments) of convoluted functions.

By the late 1960s the use of line breadths had largely been discarded in favour of the more powerful Fourier (Warren–Averbach), variance and related methods. Provided that the data are of high quality and due allowance is made for systematic errors (Section 2), these methods give a wealth of detailed and accurate information about microcrystalline properties. Size broadening gives the mean dimension of crystallites or domains in various directions and hence provides information about their shape, and the distribution of size can be obtained. The 'size' contribution can also be interpreted in terms of various types of mistake—deformation and twin faults in metals, arising from a misplacement of successive layers of atoms, mistakes due to the more or less random rotation of layers in turbostratic structures, and due to a change in the interlayer spacing at random intervals—and information on the nature and density of dislocations can be extracted. The variance method gives the r.m.s. strain (cf. equation 2) and details of the variation of strain within crystallites or domains can be found from the Fourier coefficients. A comprehensive survey of the procedures for applying both methods and the interpretation of the results has been carried out by Klug and Alexander (1974, ch. 9; see also Warren 1969). Of the two methods, the Fourier approach is the more rigorous, since no assumptions are made about the nature of the intensity distribution when correcting for instrumental effects. In practice the distinction may be unimportant, due to the presence of systematic errors (Section 2), and in any event the two methods can be regarded as complimentary. The application of the Fourier and variance methods in general requires that the diffraction lines are well resolved and is thus restricted to materials with high symmetry or which exhibit a high degree of preferred orientation. Most materials, on the other hand, including many of technological importance, such as ceramics, some catalysts and polymers, have complex patterns with severe overlapping of peaks. Significant advances during the last decade or so in pattern-decomposition methods, whereby a suitable model is fitted to the total diffraction pattern to give the characteristics of individual lines, means that a study of any crystalline material or mixture of substances is now feasible. Analyses are based on the FWHM and integral breadth of each line and, with modifications, the methods of early workers, based on assumed line shapes, have been given a new lease of life (Section 3). The Fourier and variance methods remain the best technique in cases where they are applicable, but otherwise line-broadening analysis by means of total pattern fitting can give valuable, if less accurate, information on crystal imperfections.

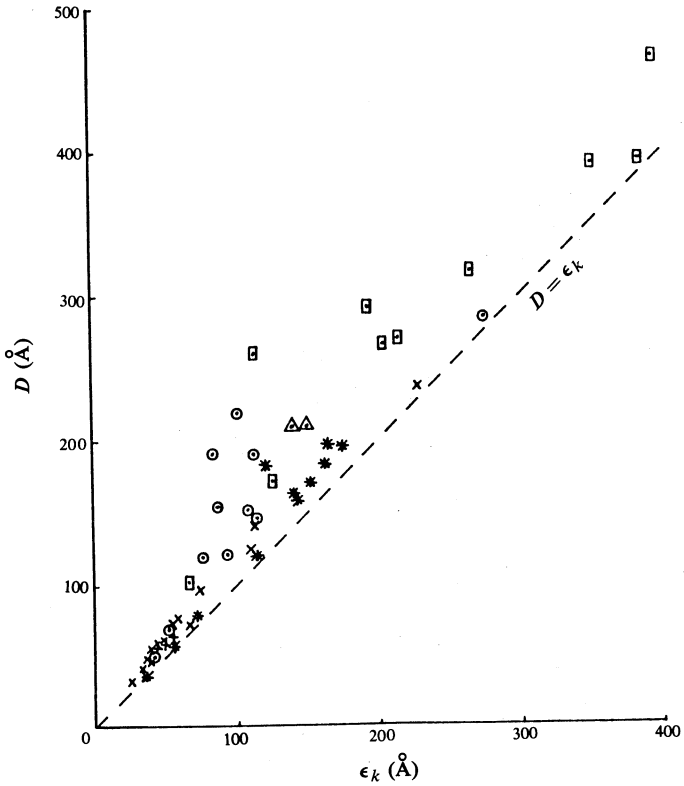

Fig. 1. Comparison between estimates of the apparent crystallite size determined by the Fourier (Warren–Averbach) analysis (D) and the variance method (ϵ_k): circles, Langford (1965, 1968), Louër *et al.* (1972); triangles, Halder and Wagner (1966); crosses, Guillatt and Brett (1970, 1971); squares, Mignot and Rondot (1973); pluses, Niepce *et al.* (1978); and stars, Le Bail and Louër (1980).

2. Sources of Error in Line Profile Analysis

As noted above, the Fourier and variance methods for line-broadening analysis only give reliable and accurate information about structural imperfections if the effects of random and systematic errors are taken into account; either they must be minimised or a correction must be made. There is evidence to suggest that this has not always been done in the past. For example, in theory both methods give the same measure of size, namely the area-weighted mean thickness of crystallites or domains measured in a direction perpendicular to the diffracting planes (Wilson 1962), but Langford (1968) noted a significant discrepancy between the size ϵ_k given by the variance and that obtained from the Fourier cosine coefficients (D) for nickel powder. The difference can only arise in the analysis of the experimental data and Le Bail (1976) made a survey of values of ϵ_k and D reported in the literature by several authors and for a wide range of samples. His findings are summarised in Fig. 1, where it can be seen that the 'Fourier size' is always greater than the 'variance size', sometimes by a factor of two or more. It is now known that this discrepancy is largely due to truncation of line profiles at finite range and that it depends critically on the method used for determining the initial slope of the $A(n)$ versus n curve (Delhez *et al.* 1986).

The effect of truncation is to *reduce* the estimate of ϵ_k, the fractional decrease being approximately equal to the fraction of intensity 'lost' by truncation, typically about 5% (Langford 1982). The size D is *increased* by a somewhat greater amount and there may also be an appreciable error in the strain value (Delhez *et al.* 1988).

(a) Errors in the Fourier Method

The principal sources of error in the Fourier/Warren–Averbach analysis are:

(a) counting statistics;
(b) standard used to obtain g profiles;
(c) background determination;
(d) truncation of profiles at finite range;
(e) sampling interval (step length);
(f) choice of origin; and
(g) limitations of approximations used in analysis.

These affect the analysis in different ways and by differing amounts. Young *et al.* (1967) simulated the effects of (c), (d) and (e) and many authors have since discussed the treatment of errors in the Fourier method. For example, Delhez *et al.* (1980, 1982) have given corrections for (a), (b) and (f). Procedures for improving the reliability of line profile analysis by the Fourier method are presented by Zorn (1988, present issue p. 237) and Delhez *et al.* (1988, p. 213).

(b) Errors in the Variance Method

Many of the sources of error listed above apply equally to the variance approach, except that the origin is always taken as the centroid of the peak and any error in its position has negligible effect, and the choice of step length is less critical. The method is based on the assumption that the intensity falls to zero as the inverse square of the range in the profile tails. The variance W then varies linearly with the range of integration σ (Wilson 1962), or

$$W = W_0 + k\sigma. \tag{5}$$

The level and slope of the background subtracted from the peak are adjusted until an optimum fit of (5) is obtained (Langford and Wilson 1963). These parameters define what may be regarded as the 'true' background under the peak for the purposes of line-broadening analysis, and they can be used to advantage for making a truncation correction in the Fourier method.

In order to correct for the unavoidable truncation of a profile at finite range, some function must be used to allow for the missing 'tails'. In practice the same inverse-square variation as leads to (5) is used and the corrections to be subtracted from W_0 and k are then $W_0\, k/\sigma_{\max}$ and $k^2/\sigma_{\max}$ respectively. Also, the total integrated intensity S_∞, equivalent to the cosine coefficient $A(0)$ multiplied by the range in the Fourier approach, is given by

$$S_\infty = S_{\sigma_{\max}}/(1 - k/\sigma_{\max}), \tag{6}$$

where $S_{\sigma_{\max}}$ is the integrated intensity of the profile at maximum range. It should be noted that in theory the intensity never falls to zero, but is a minimum half-way

between successive reflections (Delhez *et al.* 1986). However, in practice the above assumption is adequate for the purpose of making a correction for truncation and in any event for a powder sample other peaks will occur between successive orders. An analogous assumption is made when correcting for truncation in the Fourier method (Delhez *et al.* 1986). A correction procedure is currently being developed and it remains to be seen how this will affect the detailed information on strain which can be extracted by this method.

There are two other corrections, for non-additivity and curvature, which do not occur in the Fourier approach. While the additive property of variances holds if the constituent profiles extend to infinity, some instrumental functions fall to zero at a finite range and a small non-additivity correction is required. Also, there is a slight residual curvature of the variance-range function (5), for which a correction is again made. Systematic errors in the variance method have been summarised by Langford (1982).

3. Line Profile Analysis from Total Pattern Fitting

The resolution of a powder pattern into its constituent Bragg reflections is carried out in two stages. First a peak search is carried out to ascertain the positions of all lines of the pattern, eliminating 'false' peaks due to statistical noise (Huang 1988, present issue p. 201), and then the parameters for individual profiles are obtained and refined. Various models have been used for the latter. For example, the convolution of several Cauchy functions was preferred by Parrish *et al.* (1976), to give deconvoluted f profiles. Langford *et al.* (1986) used the pseudo-Voigt or Pearson VII functions, with allowance for asymmetry of the experimental profiles. A promising approach, intended for Rietveld refinement but equally applicable to line-broadening analysis, is the non-analytical 'learned peak-shape function' introduced by Hepp and Baerlocher (1988, present issue p. 229), in which an optimum fit is achieved. Langford (1987) has reviewed pattern-decomposition methods and other procedures for total pattern fitting. The aim of pattern decomposition in this context is to obtain reliable estimates of line-profile parameters, particularly the position, height, area and breadth (FWHM) of each peak, for use in an analysis of structural imperfections. There are currently two ways in which this can be carried out; in the first it is assumed that the line profiles approximate to Voigt curves, the convolution of Cauchy and Gaussian functions (Langford 1978) and in the second approach a direct analysis of the breadth parameters, given by pattern decomposition, is carried out (Keijser *et al.* 1983).

(a) Voigt Analysis of Line Breadths

After finding the breadths of individual lines, correction must be made for instrumental effects, if this is not included in the pattern decomposition, and the corrected breadths are then separated into order-independent ('size') and order-dependent ('strain') components. There are thus two stages of deconvolution to be carried out. Now instrumental profiles have Cauchy-like (inverse-square) tails, if the data are obtained with a conventional angle-dispersive X-ray diffractometer, and the g profiles will tend to be Gaussian if obtained from synchrotron or continuous-neutron sources. The tails of the line profile due to small crystallites are dominated by an inverse-square term, though the precise nature of the profile depends on the shape of the crystallites and the distribution of size, and in general strain profiles tend to be

Gaussian. There is thus both theoretical and experimental evidence to support the use of the Voigt function for the purpose of deconvolution in line-profile analysis. In the following it is assumed that the equivalent Voigt function has the same peak height, area and FWHM as the experimental line profile.

The Voigt function can be expressed as (Langford 1978, equation 22)

$$I(x) = \mathrm{Re}[\beta_C I_C(0)\,\omega\{\pi^{\frac{1}{2}} x/\beta_G + \mathrm{i}\,k\}], \tag{7}$$

where β_C and β_G are the integral breadths of the Cauchy and Gaussian components, $I_C(0)$ and $I_G(0)$ are their peak heights, $k = \beta_C/\pi^{1/2}\beta_G$ and $\omega\{z\}$ is the complex error function. If it is assumed that the experimental line profiles can be represented by a Voigt curve, then their constituent Cauchy and Gaussian components can be found and deconvoluted in the usual way (equations 16 and 17). In general the Voigt model fits experimental data well at intermediate and high angles and is usually adequate at low angles, provided that the lines are reasonably symmetrical (Langford 1987). [The error introduced by asymmetry has been considered by Keijser *et al.* (1982).]

Before embarking on a Voigt analysis of the data, the *Voigt parameter* ϕ, the ratio of the FWHM to the integral breadth, is obtained for each line in the g and h patterns. (If Kα radiation is used, then the Kα_2 component must be removed before obtaining the breadths.) The Voigtian can only be considered as a suitable model if

$$\underset{\text{(Cauchy limit)}}{2/\pi\ (=0{\cdot}6366)} \leqslant \phi \leqslant \underset{\text{(Gaussian limit)}}{2(\ln 2/\pi)^{\frac{1}{2}}\ (=0{\cdot}9394)}. \tag{8}$$

Values of ϕ slightly less than $2/\pi$ can occur with high-resolution instrumental functions, which are usually assumed to be Cauchy. Data with $\phi > 0{\cdot}9394$ are suspect.

Cauchy and Gaussian Components: The Cauchy and Gaussian integral breadths are obtained from the experimental values of β and ϕ for the g and h profiles. Fractional components β_C/β can be found by interpolation from Table 1 or graphically from Fig. 2. Alternatively, approximate values of the constituent breadths, accurate to within 1%, are more conveniently given by (Keijser *et al.* 1982, equations 3–5)

$$\beta_C = \beta(2{\cdot}0207 - 0{\cdot}4803\phi - 1{\cdot}7756\phi^2), \tag{9}$$

$$\beta_G = \beta\{0{\cdot}64420 + 1{\cdot}4187(\phi - 2/\pi)^{\frac{1}{2}} - 2{\cdot}2043\phi + 1{\cdot}8706\phi^2\}. \tag{10}$$

Voigt Parameters from β_C and β_G: If β_C and β_G are known, the corresponding Voigt function, aside from a scale factor which depends on the peak heights of the component functions, can be obtained from (7). The integral breadth is given by (Langford 1978, equation 25)

$$\beta = \beta_G \exp(-k^2)/\{1 - \mathrm{erf}(k)\} \tag{11}$$

Table 1. Fractional Cauchy and Gaussian components of the integral breadth of a Voigt function for values of the Voigt parameter ϕ in the range $2/\pi \leqslant \phi \leqslant 2(\ln 2/\pi)^{1/2}$

ϕ	β_C/β	β_G/β	ϕ	β_C/β	β_G/β
0·6464	0·9698	0·1403	0·6709	0·8975	0·2665
0·6469	0·9685	0·1438	0·6740	0·8888	0·2786
0·6474	0·9667	0·1474	0·6774	0·8789	0·2917
0·6480	0·9654	0·1513	0·6812	0·8678	0·3060
0·6486	0·9634	0·1553	0·6854	0·8550	0·3216
0·6492	0·9612	0·1595	0·6903	0·8405	0·3387
0·6499	0·9593	0·1640	0·6961	0·8240	0·3576
0·6507	0·9568	0·1687	0·7026	0·8050	0·3785
0·6516	0·9544	0·1737	0·7099	0·7832	0·4017
0·6525	0·9518	0·1790	0·7184	0·7579	0·4276
0·6535	0·9489	0·1846	0·7282	0·7282	0·4565
0·6546	0·9454	0·1905	0·7397	0·6935	0·4891
0·6557	0·9423	0·1969	0·7530	0·6525	0·5259
0·6570	0·9383	0·2036	0·7681	0·6038	0·5678
0·6585	0·9341	0·2108	0·7866	0·5456	0·6157
0·6600	0·9295	0·2185	0·8079	0·4756	0·6708
0·6617	0·9242	0·2267	0·8326	0·3906	0·7346
0·6636	0·9187	0·2356	0·8628	0·2868	0·8090
0·6658	0·9123	0·2451	0·8977	0·1589	0·8965
0·6682	0·9054	0·2554	0·9395	0·0000	1·0000

or by the approximation of Keijser *et al.* (equation 6):

$$\beta = \beta_G/\{-\tfrac{1}{2}\pi^{\frac{1}{2}}k+\tfrac{1}{2}(\pi k^2+4)^{\frac{1}{2}}-0{\cdot}234k\exp(-2{\cdot}176k)\}. \tag{12}$$

The FWHM $2w$, given by (Langford 1978, equation 27)

$$\mathrm{Re}\{\omega(\pi^{\frac{1}{2}}w/\beta_G+\mathrm{i}\,k)\} = \beta_G/2\beta, \tag{13}$$

can be obtained from the approximation for ϕ devised by Ahtee *et al.* (1984, equation 7):

$$\phi = 2(\ln 2/\pi)^{\frac{1}{2}}(1+0{\cdot}9039645k+0{\cdot}7699548k^2)/(1+1{\cdot}346216k+1{\cdot}136195k^2). \tag{14}$$

Correction for Instrumental Broadening: From (3), if $f(x)$, $g(x)$ and $h(x)$ are assumed to be Voigtian, then

$$h = h_C \star h_G = f_C \star f_G \star g_C \star g_G. \tag{15}$$

The Cauchy and Gaussian components of the integral breadths of $g(x)$ and $h(x)$ are obtained from $\beta_g, \phi_g, \beta_h, \phi_h$ by means of Table 1, Fig. 2 or equations (9) and (10), and the corresponding breadths of $f(x)$ are given by

$$\beta_{fC} = \beta_{hC}-\beta_{gC}, \tag{16}$$

$$\beta^2_{fG} = \beta^2_{hG}-\beta^2_{gG}. \tag{17}$$

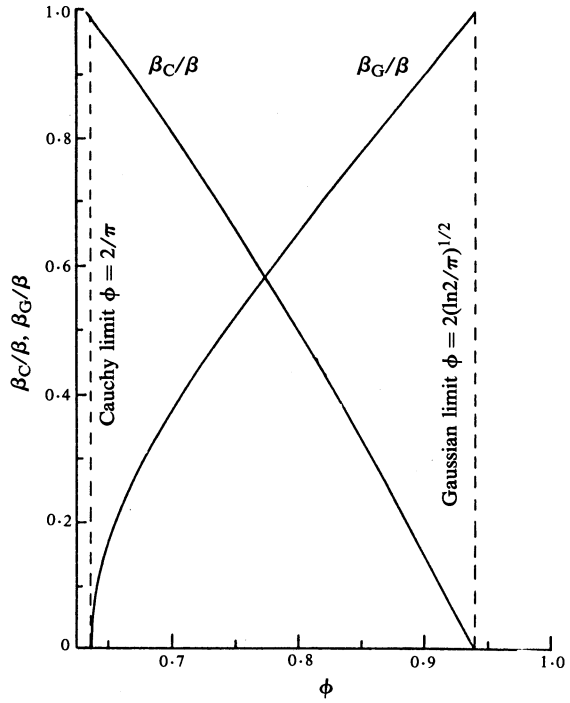

Fig. 2. Variation of the fractional Cauchy and Gaussian components of the integral breadth of a Voigt function (β_C/β and β_G/β) with the Voigt parameter ϕ (=FWHM/β).

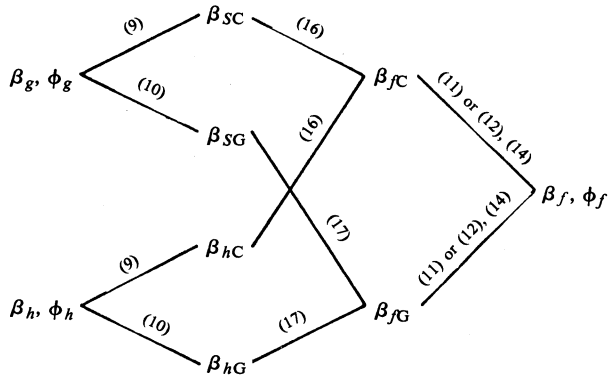

Fig. 3. Procedure for correcting the breadths of the broadened (h) profiles for instrumental effects by the Voigt method.

The breadths β_{fC} and β_{fG} can be combined to give the integral breadth β_f of $f(x)$, from (11) or (12). If required ϕ_f, and hence $2w_f$, is given by (14). This procedure is summarised in Fig. 3.

Size–Strain Separation: Size–strain analysis, which amounts to a separation of the order-independent and order-dependent contributions to the f profiles followed

by the application of (1) and (2), is carried out in three stages: (a) Williamson–Hall plot; (b) multiple-line analysis; and (c) single-line analysis.

(a) *Williamson–Hall plot:* The graph of $\beta_f \cos\theta$ versus $\sin\theta$ (breadths in units of 2θ) or β_f versus $1/d$ (breadths in reciprocal units) gives a useful visual indication of the nature of any imperfections present in the sample, since the slope depends on strain and the intercept varies as the reciprocal of the size of the crystallites or domains. [It should be noted that Williamson and Hall (1953) also used a plot of β_f^2 versus $1/d^2$.] It is possible to tell at a glance if strain is significant, whether the crystallite shape is anisotropic, or the nature of any mistakes present (Langford 1968; Langford *et al.* 1986). However, since Cauchy functions are implied for both size and strain contributions, the plot should not be used quantitatively.

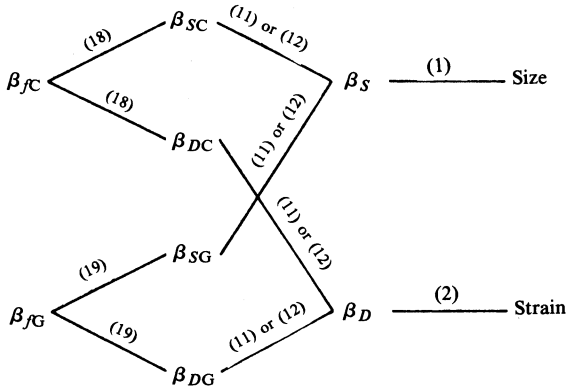

Fig. 4. Procedure for multiple-line size–strain analysis by the Voigt method.

(b) *Multiple-line analysis:* If *reliable* data are available for two or more orders of a reflection and the order-independent ('size') and order-independent ('strain') profiles are assumed to be Voigtian, then the Cauchy contributions β_{SC} and β_{DC} are obtained from

$$\beta_{fC} \cos\theta = \beta_{SC} + \beta_{DC} \sin\theta \quad (\beta_{fC} \text{ in } 2\theta) \tag{18a}$$

or

$$\beta_{fC} = \beta_{SC} + \beta_{DC}/d \quad (\beta_{fC} \text{ in reciprocal units}), \tag{18b}$$

and the Gaussian contributions β_{SG} and β_{DG} from

$$\beta_{fG}^2 \cos^2\theta = \beta_{SG}^2 + \beta_{DG}^2 \sin^2\theta \quad (\beta_{fG} \text{ in } 2\theta) \tag{19a}$$

or

$$\beta_{fG}^2 = \beta_{SG}^2 + \beta_{DG}^2/d^2 \quad (\beta_{fG} \text{ in reciprocal units}). \tag{19b}$$

The contributions β_{SC} and β_{SG} are combined by means of (11) or (12) to give β_S, the order-independent part of β_f, and this can be interpreted in terms of crystallite/domain size by means of (1). Similarly, β_{DC} and β_{DG} are combined to give β_D, the order-dependent part of β_f, and the corresponding estimate of strain is given by (2). The procedure is summarised in Fig. 4.

(c) *Single-line analysis:* When a multiple-line analysis cannot be applied, because higher orders of a reflection are absent or the breadths are inaccurate, size and strain can be separated for a single line if it is assumed that the size profile is Cauchy ($\beta_D = \beta_{fC}$) and that the strain distribution is pure Gaussian ($\beta_D = \beta_{fG}$). Estimates of size and strain are then given directly by (1) and (2).

Errors in the Voigt Analysis: It should be remembered that in general the errors in any estimate of size and strain from a Voigt analysis of line breadths will be large. This is partly due to counting statistics (Langford 1980; Keijser *et al.* 1982). It is usually impracticable to spend as long counting at each step for the total pattern as it is for individual lines with the Fourier and variance methods, and random errors will in general be greater. Errors due to residual sample broadening of the g pattern can be avoided by careful preparation of the standard. Within the limitations of the assumptions made in the Voigt approach, truncation of lines is not a serious problem, since areas are calculated from analytical functions and, provided that about 8 to 10 points are recorded across the range of the half-width $2w$ for each line, errors due to sampling interval should be inappreciable. Systematic errors will be introduced by the use of approximations (9), (10) and (12) and, for Kα radiation, by the removal of the Kα_2 component, if this is done analytically (Keijser *et al.* 1982). Inadequacy of the Voigt model gives rise to a systematic error which cannot readily be quantified. While this will affect the absolute accuracy of any derived parameters, experience has shown that self-consistent relative values are given by the method. The use of the single-line approach rather than a multiple-line analysis can introduce a further systematic error, as is shown below.

(b) Direct Approach to the Analysis of Line Breadths

We assume a shape function $h(h_1, h_2, \ldots)$ for the measured profiles of the specimen investigated and a shape function $g(g_1, g_2, \ldots)$ for the instrumental profile, where $h_1, h_2, \ldots$ and $g_1, g_2, \ldots$ are parameters. In this approach there are no mathematical limitations concerning h and g; e.g. asymmetric functions are allowed. Within the scheme of the shape functions adopted, a mathematical relation between the parameters $h_1, h_2, \ldots$ and $g_1, g_2, \ldots$ and the area-weighted crystallite size D and the r.m.s. strain $\langle e^2 \rangle^{1/2}$ is obtained by the following procedure:

(i) determine analytically the Fourier coefficients $H(n, h_1, h_2, \ldots)$ and $G(n, g_1, g_2, \ldots)$ of h and g normalised so that $H(n=0) = G(n=0) = 1$, n being the harmonic number;

(ii) obtain the Fourier coefficient F of the pure structurally broadened profile in terms of $n, h_1, h_2, \ldots, g_1, g_2, \ldots$ by application of Stokes' procedure (1948),

$$F(n, h_1, h_2, \ldots, g_1, g_2, \ldots) = A^f + \mathrm{i}\, B^f = \frac{H(n, h_1, h_2, \ldots)}{G(n, g_1, g_2, \ldots)}; \tag{20}$$

(iii) express in terms of $h_1, h_2, \ldots$ and $g_1, g_2, \ldots$

$$D = -dl\left(\left| \frac{\mathrm{d}A^f}{\mathrm{d}n} \right|_{n \to 0} \right)^{-1}, \tag{21}$$

$$\left| \frac{\mathrm{d}^2 A^f}{\mathrm{d}n^2} \right|_{n \to 0} = \left| \frac{\mathrm{d}^2 A^S}{\mathrm{d}n^2} \right|_{n \to 0} - 4\pi^2 l^2 \langle e^2 \rangle, \tag{22}$$

where A^S is the Fourier coefficient of the size-broadened profile, d is the interplanar spacing and l is the order of the reflection.

According to (21), D can be determined from a single line, whereas, from (22), $\langle e^2 \rangle^{1/2}$ [and $\mathrm{d}^2 A^S(n)/\mathrm{d}n^2$] can be determined from two orders of a reflection. Because the profile fits are different for different orders, the reliability of a multiple-line method on the basis of (21) and (22) is very limited and results may be misleading. However, if the size estimates, from separate orders, according to (21), coincide, a reliable strain value might be obtained.

In view of the above a single-line analysis will be appropriate in many cases and is unavoidable if multiple orders are absent. In the single-line approach an additional assumption is required about the term $|\mathrm{d}^2 A^S/\mathrm{d}n^2|_{n \to 0}$ in (22) (for details see Keijser *et al.* 1983). Some profile-shape functions are unsuitable for use with this direct approach, as their mathematical properties are incompatible with (21) and/or (22). Gaussian and generally Pearson VII functions do not conform to (21) because the derivative of the Fourier transform for $n \to 0$ is always zero, implying that D is infinite. The use of this approach with Voigt and pseudo-Voigt shape functions has been described by Keijser *et al.* (1983).

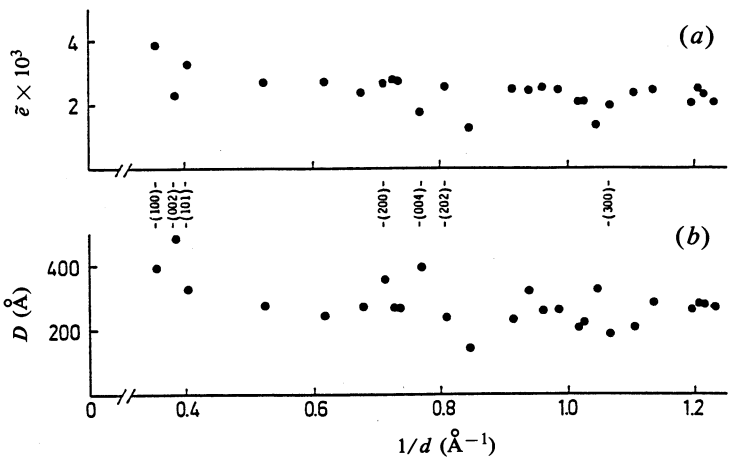

Fig. 5. Estimates for ZnO of (*a*) the strain and (*b*) the size against $1/d$ obtained by the single-line method (from Sonneveld *et al.* 1986).

4. Example of Line Profile Analysis from Total Pattern Fitting

As an example of estimating crystallite size and strain by total pattern fitting, data obtained from a sample of ZnO (ZnO-B of Langford *et al.* 1986) will be considered. The Pearson VII function, with allowance for asymmetry, was used to model the individual peaks of the pattern. The results of applying a single-line Voigt analysis are shown in Fig. 5 (see also Table 1 of Sonneveld *et al.* 1986). For reflections of which multiple orders are present, single-line and multiple-line analyses may be compared in Table 2 and Fig. 6. Clearly the largest size and smallest strain values are observed for the (002) and (004) reflections [see below for (006)]. For the other reflections no

Table 2. Comparison of size and strain values for ZnO obtained from single-line and multiple-line analyses (Sonneveld *et al.* 1986)

hkl	Size D (Å)		Strain $\tilde{e}\times10^3$	
	Multiple	Single	Multiple	Single
(100)		392		3·8
(*h*00) (200)	318	352	2·9	2·7
(300)		186		1·9
(101)		327		3·3
(*h*0*h*)	305		3·2	
(202)		238		2·5
(002)		484		2·3
(00*l*)	417		2·0	
(004)		391		1·7

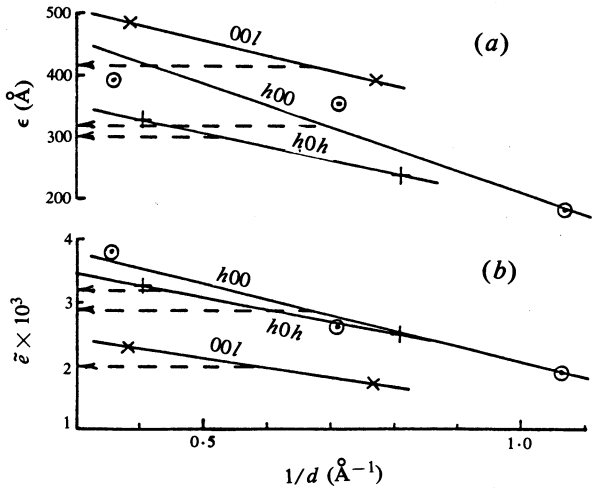

Fig. 6. Comparison between (*a*) size and (*b*) strain for ZnO estimated by single-line (*solid*) and multiple-line (*dashed*) methods.

distinct anisotropy with respect to size and strain is apparent (Fig. 5). These results are similar to those obtained for a ZnO powder which only exhibited size broadening (ZnO-A of Langford *et al.* 1986), where the more accurate Fourier and variance methods were applied.

As regards the accuracy of the results obtained, the quality of fit in this example for the Pearson VII function, can be assessed from the factors R_p and R_{wp} (Young *et al.* 1982). From the values of these factors for the ZnO sample (Langford *et al.* 1986, Table 3), it is evident that the accuracy is lowest at high angles, where the intensity of lines tends to be low and, in this case, there is more peak overlap. This suggests that, for size–strain analysis in conjunction with pattern fitting, in many cases size and strain data can be obtained by performing a single-line analysis on lines considered to be fitted best. This is corroborated by the fact that, in this example, a combination of (002), (004) *and* (006) in a multiple-line analysis gives physically unrealistic results. [However, it should be noted that the (006) has a very low intensity.]

In the particular case of size and strain broadening being Voigtian in character, and if (1) and (2) hold for their Cauchy and Gaussian components, then the following trends are to be expected if a single-line analysis is applied to different orders of a reflection:

(a) Since it is assumed that $\beta_S = \beta_{fC}$, a Gaussian order-independent component is ignored and a Cauchy order-dependent part is included. The estimate of β_S thus increases with $1/d$ (or angle) and the estimated size decreases (Table 2).

(b) By assuming that $\beta_D = \beta_{fG}$, a Cauchy order-dependent component is ignored and an order-independent Gaussian contribution is included. The estimate of β_D, and hence the estimated strain, then decreases with $1/d$ (Table 2).

The effect of these tendencies is strikingly apparent from Fig. 6 and in this particular example the size and strain values given by the two methods differ by up to 30%. The trend is also evident for both size and strain values in Fig. 5. However, the sign and magnitude of systematic errors introduced by applying the single-line approach cannot readily be assessed; for size estimated from the Cauchy component of the total profile, an unknown strain contribution is included, but the unknown size contribution to the Gaussian component is ignored.

Further, in a multiple-line analysis, the error in values for size and strain is in general governed by that order of a reflection for which the quality of the breadth parameters is lowest. Also, no information is normally available about the precise shape of the size and strain component profiles, i.e. whether or not the Voigtian is in fact a close approximation. No general statement can therefore be made regarding the accuracy of size–strain data obtained from a single-line analysis, compared with that from a multiple-line approach based on assumed profile shapes.

References

Ahtee, M., Unonius, L., Nurmela, M., and Suortti, P. (1984). *J. Appl. Cryst.* **17**, 352–7.
Averbach, B. L., and Warren, B. E. (1949). *J. Appl. Phys.* **20**, 885–6.
Delhez, R., Keijser, Th.H. de, and Mittemeijer, E. J. (1980). *In* 'Accuracy in Powder Diffraction', NBS Spec. Pub. No. 567 (Eds S. Block and C. R. Hubbard), pp. 213–53 (NBS: Washington, DC).
Delhez, R., Keijser, Th.H. de, and Mittemeijer, E. J. (1982). *Fresenius Z. Anal. Chem.* **312**, 1–16.
Delhez, R., Keijser, Th.H. de, Mittemeijer, E. J., and Langford, J. I. (1986). *J. Appl. Cryst.* **19**, 459–66.
Delhez, R., Keijser, Th.H. de, Mittemeijer, E. J., and Langford, J. I. (1988). *Aust. J. Phys.* **41**, 213–27.
Guillatt, I. F., and Brett, N. H. (1970). *Philos. Mag.* **21**, 671–80.
Guillatt, I. F., and Brett, N. H. (1971). *Philos. Mag.* **22**, 647–53.
Halder, N. C., and Wagner, C. N. J. (1966). *Adv. X-ray Anal.* **9**, 91–102.
Hall, W. H. (1949). *Proc. Phys. Soc. London* A **62**, 741–3.
Hepp, A., and Baerlocher, Ch. (1988). *Aust. J. Phys.* **41**, 229–36.
Huang, T. C. (1988). *Aust. J. Phys.* **41**, 201–12.
Keijser, Th.H. de, Langford, J. I., Mittemeijer, E. J., and Vogels, A. B. P. (1982). *J. Appl. Cryst.* **15**, 308–14.
Keijser, Th.H. de, Mittemeijer, E. J., and Rozendaal, H. C. F. (1983). *J. Appl. Cryst.* **16**, 309–16.
Klug, H. P., and Alexander, L. R. (1974). 'X-ray Diffraction Procedures for Polycrystalline and Amorphous Materials', 2nd edn (Wiley: New York).
Langford, J. I. (1965). *Nature* **207**, 966–7.
Langford, J. I. (1968). *J. Appl. Cryst.* **1**, 131–8.
Langford, J. I. (1978). *J. Appl. Cryst.* **11**, 10–14.

Langford, J. I. (1980). *In* 'Accuracy in Powder Diffraction', NBS Spec. Pub. No. 567 (Eds S. Block and C. R. Hubbard), pp. 255–69 (NBS: Washington, DC).
Langford, J. I. (1982). *J. Appl. Cryst.* **15**, 315–22.
Langford, J. I. (1987). *Prog. Cryst. Growth Charact.* **14**, 185–211.
Langford, J. I., Louër, D., Sonneveld, E. J., and Visser, J. W. (1986). *Powder Diffraction* **1**, 211–21.
Langford, J. I., and Wilson, A. J. C. (1963). *In* 'Crystallography and Crystal Perfection' (Ed. G. N. Ramachandran), pp. 207–22 (Academic: London).
Le Bail, A. (1976). Thesis, University of Rennes.
Le Bail, A., and Louër, D. (1980). *Rev. Chimie Min.* **17**, 522–32.
Louër, D., Weigel, D., and Langford, J. I. (1972). *J. Appl. Cryst.* **5**, 353–9.
Mignot, J., and Rondot, D. (1973). *J. Appl. Cryst.* **6**, 447–56.
Niepce, J.-C., Watelle, G., and Brett, N. H. (1978). *J. Chem. Soc.* **74**, 1530–7.
Parrish, W., Huang, T. C., and Ayers, G. L. (1976). *Trans. Am. Cryst. Soc.* **12**, 55–73.
Scherrer, P. (1918). *Nachr. Ges. Wiss. Göttingen*, 26 Sept., 98–100.
Sonneveld, E. J., Delhez, R., Keijser, Th.H. de, Langford, J. I., Mittemeijer, E. J., Visser, J. W., and Louër, D. (1986). Proc. 12th Conf. on Applied Crystallography, pp. 26–31 (Silesian University: Katowice).
Stokes, A. R. (1948). *Proc. Phys. Soc. London* **61**, 382–91.
Stokes, A. R., and Wilson, A. J. C. (1944). *Proc. Phys. Soc. London* **56**, 174–81.
Tournarie, M. (1956). *C. R. Acad. Sci. Paris* **242**, 2016–18; 2161–4.
Van Arkel, A. E. (1925). *Physica* **5**, 208–12.
Warren, B. E. (1969). 'X-ray Diffraction' (Addison–Wesley: Reading, Mass.).
Warren, B. E., and Averbach, B. L. (1950). *J. Appl. Phys.* **21**, 595–9.
Williamson, G. K., and Hall, W. H. (1953). *Acta Metall.* **1**, 22–31.
Wilson, A. J. C. (1962). *Nature* **193**, 568–9.
Wilson, A. J. C. (1962). 'X-ray Optics', 2nd edn (Methuen: London).
Young, R. A., Gerdes, R. J., and Wilson, A. J. C. (1967). *Acta Cryst.* **22**, 155–62.
Young, R. A., Prince, E., and Sparks, R. A. (1982). *J. Appl. Cryst.* **15**, 357–8.
Zorn, G. (1988). *Aust. J. Phys.* **41**, 237–49.

Manuscript received 7 January, accepted 15 February 1988